Membrane fouling in reverse-osmosis filters during real drinking water purification: Impact of operation modes and pretreatment

Bifeng Zhang, Yijuan Jiang, Fang Fang, Kaisong Zhang*

*Key Laboratory of Urban Pollutant Conversion, Institute of Urban Environment, Chinese Academy of Sciences, Xiamen 361021, China,
Tel. +86 592 6190534, email: bfzhang@iue.ac.cn (B.F. Zhang), yjjiang@iue.ac.cn (Y.J. Jiang), ffang@iue.ac.cn (F. Fang),
Tel. +86 592 6190782, email: kszhang@iue.ac.cn (K.S. Zhang)*

ABSTRACT

Reverse osmosis (RO) is the most widely-used technology in drinking water purifiers. The potential membrane fouling has aroused broad attentions to the safety of drinking water. Thus, we studied the fouling of spiral wound RO filter in commercial drinking water purifiers. The feed water was treated by the sequential filtration of polypropylene filter, granular activated carbon filter, polypropylene filter, RO membrane filter, and post positional activated carbon filter. Membranes operating under different intermittent operating conditions (6, 12 and 24 h/d) were autopsied after 90 d. The formation and spatiotemporal development of fouling layer was also studied after different operation time (7, 15, 30, 45 and 90 d). The results showed biofouling formed after 7 d with increase of the fouling layer as the intermittent operation time or total operation time increased. The biochemical components of the fouling were dominated by nucleic acids and proteins under different intermittent operating conditions or time. Biofouling first occurred, followed by the combination of biological and non-biological fouling. The permeate flux of the purifier recovered to the initial level with new pretreatment filters after 85 d and thus stresses the importance of in-time replacement of pretreatment filters in commercial drinking water purifiers.

Keywords: Reverse osmosis; Fouling; Drinking water purification; Surface-enhanced Raman spectroscopy; Biochemical component

1. Introduction

An increasing occurrence of drinking water pollution has aroused broad attentions to potential safety concerns of drinking water [1]. Household purifier, as a handy and effective appliance to supply drinking water, has prevailed recently. The retail sales reached $34.5 billion in 2015 and could reach up to $187 billion by 2020 in China [2]. The global water purifier market is expected to increase by double digits during 2013–2019 [3]. Four commonly-used water purification technologies include reverse osmosis (RO), ultra filtration (UF), activated carbon (AC), and nano-filtration (NF). Among them, RO has become the dominant technology with increasing market share in recent years (Fig. 1). Nevertheless, the market scope of RO water purifiers remains huge. The most daunting challenge of purifier popularization is the maintenance after long time operation. Therefore, in-time replacements of filters are essential to avoid secondary pollution and ensure the safety of purified water.

A major impasse in membrane operation is fouling [4,5], including colloidal fouling, scaling, organic fouling, and biofouling [6]. The design of "spiral wound" elements makes membranes prone to contaminants adhesion [7]. Membrane fouling causes a decrease in membrane permeability, increases the cleaning frequency, shortens membrane service lifetime, and thus increases operation cost [8].
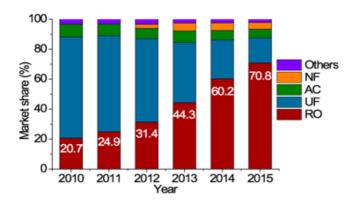
*Corresponding author.

Fig. 1. Market share of purification technology used in water purifiers [2].

Simplified laboratory systems using one or a few bacterial strains, model foulants, synthetic wastewater as the feed water or ignoring the pretreatment process were set up to monitor fouling in UF, NF or RO system [9–12]. Bacterial cells were found present in the permeate from full-scale RO membrane while absent from parallel-running test flow cells [13]. This indicates the differences in fouling between laboratory-scale test and real operating systems. The synergistic effects of foulants under complex real-world condition can not be ignored. The complex interplays of the foulants caused a higher flux decline compared with additive effects of the foulants alone [14]. Thus, fouling mechanism derived from model experiments lacks comprehensive estimation of the interactions between different types of foulants. Furthermore, present studies have mostly focused on membrane fouling during high concentration industrial or municipal wastewater treatment [15], and rarely studied the fouling during drinking water treatment.

The chemical variations within fouling layer provide hints for early-warning and dynamic changes of biofouling. Biofouling is formed by the initial bacteria attachment and subsequent reproduction and growth of attached cells [16]. The attached cells can excrete extracellular polymeric substances (EPS) that are mainly composed of organics, i.e., nucleic acids, proteins, and carbohydrates. EPS further enhance bacterial adhesion to surfaces and promotes fouling layer cohesion [17]. Surface-enhanced Raman spectroscopy (SERS) technique provides rich fingerprinting information of whole-cell related biomolecules [18]. Raman signals of molecules in close proximity to SERS-active nanoparticles (NPs) like Ag or Au NPs can be greatly enhanced by 10^6–10^{14} folds over normal Raman scattering relying on electromagnetic enhancement of these NPs [19]. Thus, highly-sensitive SERS has been successfully used for biofilms studies [20,21]. Our former studies showed that SERS was applicable to in situ monitor the fouling process of different proteins on membranes [22], dynamic changes of dominant species within biofilm formed by two model bacteria [23], and chemical variations during biofouling and cleaning of NF membranes [11].

To target potential membrane foulants during drinking water purification, commercial household drinking water purifiers using RO filters are used to investigate the actual fouling process. The permeate flux and purification efficiency are monitored to study the effect of operation conditions on membrane performance. The dynamic infrastructural changes within the fouling layer are also evaluated by SERS. To our knowledge, this is the first time that RO filters fouling is studied during tap water purification. As the safety of drinking water has attracted more and more concerns, it is essential to study the fouling development in RO filters. The study provides new insights into membrane management issues, such as, operation conditions, early-warning of membrane fouling and in-time membrane cleaning or replacement in the centralized drinking water supply.

2. Materials and methods

2.1. RO membrane test unit

Commercial drinking water purifiers containing RO membrane filters were used for fouling experiment. The detailed schematic of water purifier was shown in Fig. 2. The whole filtration system was comprised of five filters in a cascade configuration. The tap water with the conductivity of 215.7 ± 21.0 µs/cm was used as feed water. The concentration of main ions were 10.62 ± 2.92 mg/L Ca^{2+}, 1.47 ± 0.61 mg/L Mg^{2+}, and 6.61 ± 0.49 mg/L Na^+. The tap water passed through the 1st polypropylene filter (PPF) to remove the bulk impurities. The outlet water was then treated by the 2nd granular activated carbon filter (GACF) to eliminate macromolecular organic compounds, heavy metals and other harmful substances. A further removal of micro suspended solids, colloid and other granular impurities was achieved by the 3rd PPF. After that, the 4th RO filter with a filtration diameter of 0.1 nm was applied to remove organic matters, microorganisms, chemical residuals and other harmful matters. RO filtered water was stored in a pressure barrel. In front of the outlet, a post positional activated carbon filter (PACF) was used to adsorb residual color and smell. A washing system operated automatically at the beginning or during the purifier operation.

The major parameters including permeate flux and conductivity were measured and recorded every 2 d. The salt rejection was calculated according to Eq. (1).

2.2. SERS analysis

2.2.1. Synthesis of Au NPs

Oval-shaped Au NPs were synthesized according to Frens' method [24]. Briefly, 100 mL of 0.01% (wt/vol) $HAuCl_4$ solution was heated to boiling under vigorous stirring, followed by the immediate addition of 0.6 mL of 1% (wt/vol) trisodium citrate solution, and kept boiling for about 1 h. The as-prepared Au NPs have the dominant size at long axis being around 120 nm and more information about their SEM image, size distribution, and biocompatibility are described in our previous work [25,26]. Before being used for SERS enhancement, Au NPs were washed once by ultra pure water (Millipore, USA) and concentrated through centrifugation at 2900 rpm for 6 min (Eppendorf centrifuge 5430R, Germany). The supernatant was discarded, and the precipitate was collected for sample preparation.
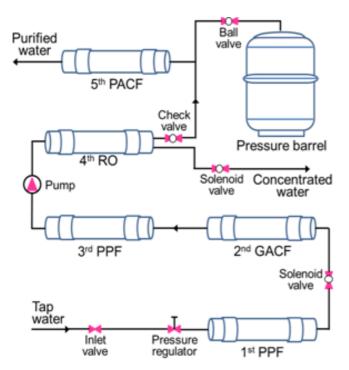
Fig. 2. Schematic outline of the drinking water purifier. (PPF: polypropylene filter, GACF: granular activated carbon filter, RO: reverse osmosis filter, PACF: post positional activated carbon filter).

2.2.2. SERS measurements

The spiral-wound RO filters were taken out at the end of each run. RO membranes were cut into wafers with a diameter of 6 mm. An equal volume of 10 µL concentrated Au NPs was dropped on the surface of membrane wafers and air-dried before SERS measurement. SERS spectra were acquired using a LabRAM Aramis (HORIBA JobinYvon) confocal micro-Raman system. Excitation was provided by a He-Ne 632.8 nm laser. A 50× objective (Olympus) with a numerical aperture of 0.55 and a working distance of 8 mm was used to focus the laser beam and collect the Raman signal. To improve the uniformity of SERS signal and minimize possible laser-induced sample damage, DuoScan in the micro-mapping mode with a scanning area of 30×30 µm² was used. Spectral acquisition time was 10 s. Five SERS spectra from five different areas of one wafer and a total of fifteen spectra from three wafers cutting from one fouled RO membrane were acquired.

2.2.3. Data pre-processing and chemometric analyses

SERS spectra were pre-processed first via baseline correction using LabSpec5 software (HORIBA JobinYvon) and then wavelet de-noising using the IrootLab toolbox (https://code.google.com/p/irootlab/) running on MATLAB 2012a [27]. Calculation of means of spectra with standard deviation, and principal component analysis-linear discriminant analysis (PCA-LDA) were performed following pre-processing via IrootLab toolbox. PCA-LDA is a combined multivariate analysis method where PCA is used to reduce the spectral variables to 10–20 factors accounting for

more than 99% of total variance and the subsequent application of LDA can derive orthogonal variables to maximize between-class variance and minimize within-class variance. Resulting PCA-LDA can be visualized as one- dimensional (1D) or two-dimensional (2D) scores plots. The nearness of plot indicates the similarity of spectra, while the distance indicates dissimilarity [27]. This facilitates the visualization of spectral variation within one class (fifteen individual spectra from one fouled membrane) or between classes (different fouled membranes).

2.3. Scanning electron microscopy (SEM) analyses

The morphology and distribution of fouling layer were characterized using a scanning electron microscopy (SEM, Hitachi S-4800, Japan). The samples were initially fixed with 2.5% glutaraldehyde in 0.1 M phosphate buffered saline for 2 h, followed by dehydration by immersing in a series of ethanol with sequential concentrations (30, 50, 70, 90 and 100%), and then critical point drying overnight (Auto-Samdri 815 Automatic Critical Point Dryer; Tousimis, Rockville, MD, USA). The dehydrated samples were then sputter coated with gold and examined by SEM.

3. Results and discussion

3.1. The effect of intermittent operation on membrane fouling and performance

To investigate the impact of intermittent operation on membrane fouling, three purifiers are operated in parallel under different intermittent operation time of 6, 12, and 24 h/d, respectively. After operating for 90 d, RO membranes were taken out and characterized. The visual inspection showed that slimy and dark-brown coloured deposits distributed over the membrane surface (Fig. 3A). SEM images of fouled membranes clearly showed different fouling degree under three intermittent operation conditions. An obvious fouling layer with rod-shaped microorganisms and their secretions appeared on RO membrane operated for 6 h/d (surface views in Fig. 3B). However, fewer microorganisms and more non-biological contaminants were observed for the prolonged operation time per day (12 or 24 h/d). The deposition of particulate matters may limit biofilm growth by occupying membrane surface [28]. Whether the microorganisms were absent or just covered by thick cake layer was still unknown. Thus, biochemical components of the fouling layer will be further analyzed in the next section. The thickness of fouling layer increased with prolonged operation time per day (cross-sectional views in Fig. 3C). This was probably due to the increasing deposition of non-biological contaminants.

Fig. 4a shows a more obvious decline in permeate flux at longer operation time per day. The normalized permeate flux remained almost unchanged (greater than 90% of initial levels) within 85 d under intermittent operation of 6 h/d and only a minor decline (30% of initial levels) was observed after 90 d. However, permeate flux declined over prolonged operation time under 12 or 24 h/d and normalized permeate flux decreased to 40% of initial levels after 90 d. The increased thickness
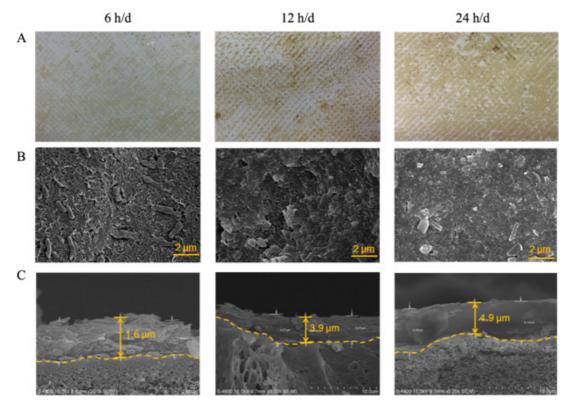
Fig. 3. Photographs (panel A), surface view (panel B) and cross-sectional view (panel C) of autopsies of fouled RO membranes operating for 90 d under intermittent operation of 6, 12, and 24 h/d respectively.
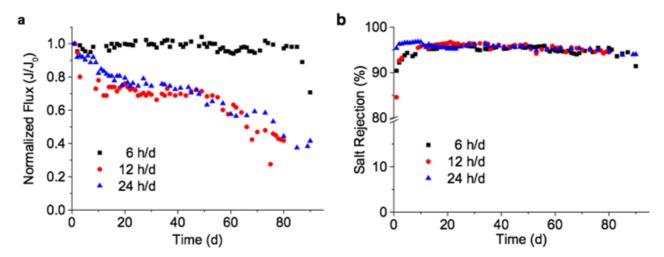

Fig. 4. Normalized flux (a) and salt rejection (b) curve upon induced fouling after RO membranes operating for 90 d under different intermittent operation of 6, 12, or 24 h/d.

of fouling layer mainly accounted for the great permeate flux decline by inducing hydraulic resistance to permeate flow and elevated trans-membrane osmotic pressure under 12 and 24 h/d (Fig. 3). The accumulated particles and colloids in the biofouling layer decrease permeate flux due to hindered back diffusion of salts from membrane surface, namely by "cake-enhanced osmotic pressure" [29–31]. Besides, synergistic effects of combined fouling layer could extremely worsen membrane permeability [14,32].

There was no significant difference in salt rejections among different intermittent operation conditions. Only small variations between 94–97% were observed over whole operation time. The related study suggested that permeate flux had small effects on salt rejection, namely "concentration effect" [33]. In most cases organic fouling even reduced diffusivity of salts through the membrane by acting as an additional barrier, thus increasing salt rejection [34,35]. Additional fouling barrier could partly counteract concentration effect which could explain the relatively stable salt rejection.

3.2. The effect of intermittent operation on membrane biofouling

Biochemical components of the fouling layer were analyzed by SERS. The heterogeneity of fouling layer would generate spectra with big variations and make it hard to analyze small chemical differences among different operation conditions. As shown in Fig. 5a, the narrow corona representing spectral variation indicated that the combination of DuoScan mode and SERS enhancement could decrease this kind of variation. Further application of PCA-LDA was used to highlight the differences of SERS spectra features between fouled membranes. Each spectrum was plotted as one point in a 2D PCA-LDA scores plot where the segregation distance was proportional to spectral dissimilarity (Fig. 5c).

Fig. 5a shows that SERS spectra of fouled membranes had few Raman bands, indicating a mild biofouling on membrane surface. Conversely, our previous study found that the enhanced biofouling experiment with a model bacterial strain had a rich chemical diversity [11]. Thus, a further investigation of membrane biofouling under real-world conditions was highly essential. The minor difference in spectra features among different intermittent operation conditions indicated that intermittent operation had small impact on biofouling (Figs. 5a and b). The band assignments and further analysis of biomolecules will be discussed below.

3.3. The effect of operation time on membrane fouling and performance

Fig. 6A shows that the colour of deposits on fouled membranes changed from light-yellow to dark-brown with prolonged operation time. SEM examination revealed an early formation of dense biofouling layer after 7 d (Fig. 6B). Bereschenko et al. [36] also observed an early biofilm structure on the surface of RO membranes within the first 4 d of flow cell operation. The fouling layer mainly comprised of microorganisms, inorganic and organic matters. Fig. 6C shows increasing fouling layer with the increase of operation time. Al-Ahmad [7] suggested that biofouling would accelerate other fouling types like scaling. This explained the early formation of biofouling and subsequent combined fouling.

Fig. 7 shows the permeate flux and salt rejection of five purifiers operating for 7, 15, 30, 45 or 90 d, respectively. The decline patterns of permeate flux were almost identical which indicated the reproducibility of fouling process among five parallel-running purifiers. A slight decline in permeate flux was observed in initial 45 d which could be due to the rapid proliferation and growth of microorganisms, as noted by SEM images (Figs. 6B and C). Subsequently, permeate flux dramatically decreased from 80% to 40% of initial levels from 45 d to 90 d. The combined fouling of microorganisms and scaling might account for this rapid decline (Fig. 6B). Nevertheless, a good performance of salt rejection varied between 92–97% was achieved over 90 days operation.

3.4. The effect of operation time on membrane biofouling

SERS spectra of fouled membranes from different operation time showed same Raman bands at 1002, 1290–1400
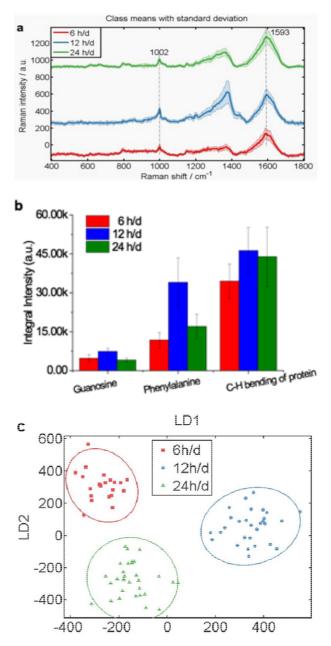

Fig. 5. SERS spectra (a), integrated Raman intensity of biomolecule bands (b) and PCA-LDA scores plots (c) of fouled RO membranes. Corona around the mean SERS spectra represents standard deviation of spectra.

and 1593 cm^{-1} (Fig. 8a). This indicated that chemical compositions were relatively fixed between different fouling layers. Previous studies also suggested that RO membrane had a selective surface for a conserved biofilm irrespective of feed water pretreatment [28] and membrane surface properties [37,38]. Nucleic acid band with guanosine-related molecule vibration at 1593 cm^{-1} [23,25] was observed. Nucleic acid are important for biofilm formation as they play unique roles in bacterial adhesion [39] and genetic information exchange [40]. Whitchurch, Tolker-Nielsen [41] found that the majority of extracellular material was not exopolysaccharide but DNA. Besides, protein bands, with ring breath of phenylal-
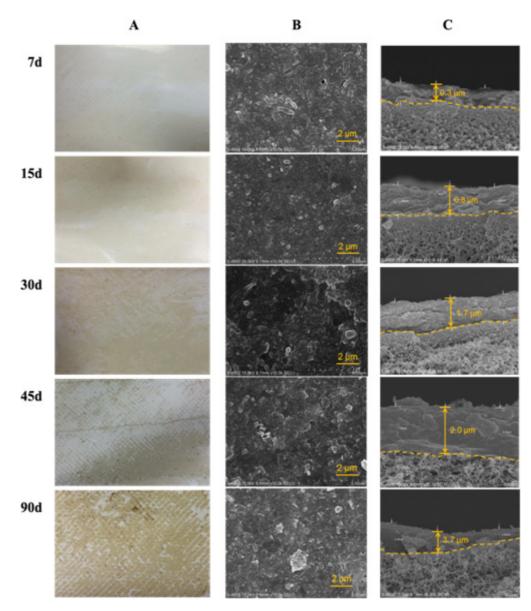
Fig. 6. Photographs (panel A), surface view (panel B) and cross-sectional view (panel C) of autopsies of fouled RO membranes operating for 7, 15, 30, 45 and 90 d.
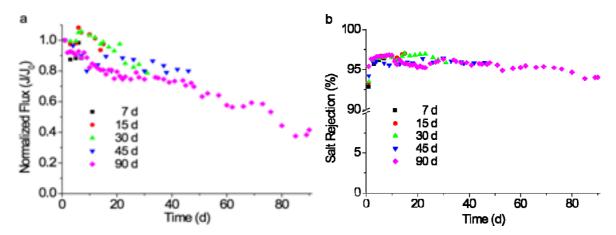

Fig. 7. Normalized flux (a) and salt rejection (b) curve of five purifiers operating for 7, 15, 30, 45 and 90 d.

anine at 1002 cm^{-1} [42] and C-H bending at 1290–1400 cm^{-1} [43], also appeared in all fouled membranes. Proteins are commonly regarded as major components contributing to membrane fouling. Many extracellular enzymes provide nutrient and energy for the biofilm by decomposing biopolymers. Besides, some non-enzymatic proteins are involved in biofilm structural integrity by constituting a link between bacterial surface and EPS [40]. The amounts of proteins were reported to far exceed carbohydrates content in biofilm matrix on a mass basis [44,45].

By contrast, SERS did not reflect significant changes in fouling layer thickness with prolonged operation time (Figs. 8a and b). The short distance enhancement of SERS only enhanced Raman signals of molecules in the close proximity to Au NPs. Thus, only chemical components on the upper layer of fouling could be detected [11]. Nevertheless, differences of SERS spectra features between these fouled membranes were extracted by the application of PCA-LDA. The PCA-LDA scores increased with prolonged operation time (Fig. 8c), consistent with the increased fouling layer (Fig. 6). As mentioned in section 3.1, it was hard to tell whether microorganisms were absent or just covered by thick cake layer. But SERS spectra showed the secretion of extracellular DNA and proteins even though there were

fewer microorganisms present on the upper layer of fouling with prolonged operation time. This indicated the existence of bacteria underneath the cake layer. Biochemical components analysis pointed out that cleaning agents for biofouling should target at nucleic acid and protein removal.

3.5. The effect of pretreatment filters on filtration performance and membrane fouling

The pretreatment filters not only impact the subsequent RO performance [46], but also affect purified water production. In order to investigate the influence of pretreatment filters on permeate flux, pretreatment filters including the 1st PPF, 2nd GACF and 3rd PPF were replaced by the new ones when normalized flux decreased to 40% of initial levels after 85 d (Fig. 7). Interestingly, the permeate flux almost recovered to initial level after the replacement (Fig. 9), indicating the great impact of pretreatment filters fouling on permeate flux. However, the permeate flux suffered the same decline pattern as before in the following operation (180 d-R2). Even so, the salt rejection was not affected by the fouling of pretreatment filters or RO membrane, and remained at a high level (92–97%). The recovered permeate flux indicated the significance of in-time pretreatment filters replacement.
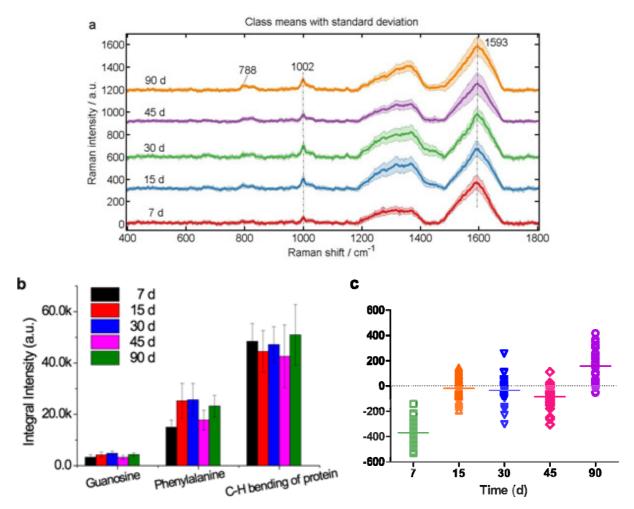

Fig. 8. SERS spectra (a), integrated Raman intensity of biomolecule bands (b) and PCA-LDA scores plots (c) of fouled RO membranes.
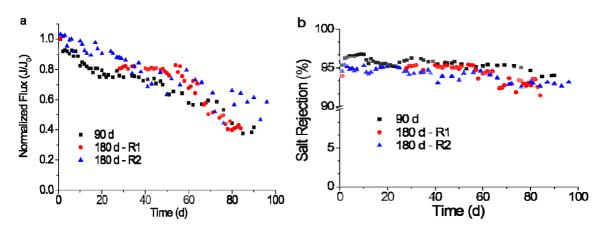
Fig. 9. Normalized flux (a) and salt rejection (b) curve of two purifiers operating for a total time of 90 d or 180 d, respectively. The pretreatment filters were replaced by the new ones when normalized flux decreased to 40% of initial levels after 85 days and corresponding data set was denoted by 180 d-R1. For ease of comparison, the data set from replaced pretreatment filters was plotted as a new start and denoted by 180 d-R2.
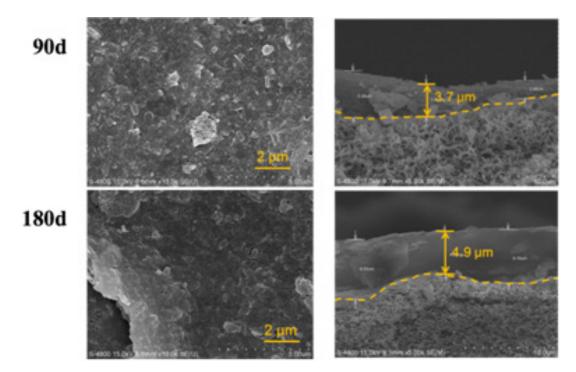

Fig. 10. Surface view (left panel) and cross-sectional view (right panel) of autopsies of fouled RO membranes after 90 and 180 d, respectively.

The fouling layer of RO membranes operated for a total time of 90 and 180 d was compared. Cross-sectional views show a significant increase in fouling layer thickness after RO membrane operated for another 90 d even with new pretreatment filters (Fig. 10). The retention effect of increased fouling layer partly contributed to the reduced permeate flux while the unaffected salt rejection. A weak protein band at 618 cm^{-1} (C-C twisting) [47] appeared after 180 days operation. Meanwhile, nucleic acid band at 788 cm^{-1} (O-P-O stretching) [48] and ring breath of phenylalanine at 1002 cm^{-1} increased (Fig. 11a). The minor differences in three main biomolecules were also observed from the integrated Raman bands intensity (Fig. 11b).

4. Conclusions

This study presented autopsy results of membrane fouling in RO filters during real drinking water purification under different operation modes. The results led to the following conclusions:

- Biofouling occurred as early as 7 d of operation. Meanwhile, the fouling layer increased with the increase of intermittent operation or operation time.
- Chemical components of fouling were almost identical among different fouling layers and were dominated by nucleic acids and proteins.
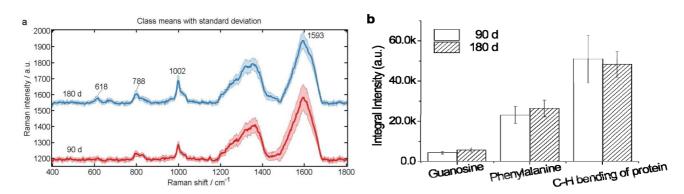
Fig. 11. SERS spectra (a) and integrated Raman intensity of biomolecule bands (b) of fouled RO membranes.

- The fouling developed with an initial biofouling phase, which was followed by a combination of biological and non-biological fouling. Therefore, more attention should be given to the pretreatment process prior to the RO filtration system to prevent biofouling problems.
- The permeate flux recovered to the initial level after 85 d operation with installation of new pretreatment filters showing the importance of in-time pretreatment filters replacement.

Acknowledgments

References

[1] D. Chalchisa, M. Megersa, A. Beyene, Assessment of the quality of drinking water in storage tanks and its implication on the safety of urban water supply in developing countries, Environ. Syst. Res., 1 (2018) 6–12.

[2] China Market Monitor Co. www.monitor.com.cn/report.aspx. 2016.

[3] B.E. Obinaju, A. Alaoma, F.L. Martin, Novel sensor technologies towards environmental health monitoring in urban environments: a case study in the Niger Delta (Nigeria), Environ. Pollut., 192 (2014) 222–231.

[4] J.S. Baker, L.Y. Dudley, Biofouling in membrane systems - A review, Desalination, 118 (1998) 81–89.

[5] H.C. Flemming, Reverse osmosis membrane biofouling, Exp. Therm. Fluid Sci., 14 (1997) 382–391.

[6] C.Y. Tang, T.H. Chong, A.G. Fane, Colloidal interactions and fouling of NF and RO membranes: a review, Adv. Colloid Interf. Sci., 164 (2011) 126–143.

[7] M. Al-Ahmad, F.A. Abdul Aleem, A. Mutiri, A. Ubaisy, Membranes in drinking and industrial water production biofuoling in RO membrane systems Part 1: Fundamentals and control, Desalination, 132 (2000) 173–179.

[8] M. Xie, W. Luo, S.R. Gray, Synchrotron fourier transform infrared mapping: A novel approach for membrane fouling characterization, Water Res., 111 (2017) 375–381.

[9] C.M. Pang, P. Hong, H. Guo, W.T. Liu, Biofilm formation characteristics of bacterial isolates retrieved from a reverse osmosis membrane, Environ. Sci. Technol., 39 (2005) 7541–7550.

[10] M. Herzberg, M. Elimelech, Physiology and genetic traits of reverse osmosis membrane biofilms: a case study with Pseudomonas aeruginosa, ISME J., 2 (2008) 180–194.

[11] L. Cui, P.Y. Chen, B.F. Zhang, D.Y. Zhang, J.Y. Li, F.L. Martin, K.S. Zhang, Interrogating chemical variation via layer-by-layer SERS during biofouling and cleaning of nanofiltration membranes with further investigations into cleaning efficiency, Water Res., 87 (2015) 282–291.

[12] T. De La. Torre, M. Harff, B. Lesjean, A. Drews, M. Kraume, Characterisation of polysaccharide fouling of an ultra filtration membrane using model solutions, Desal. Water Treat., 8 (2009) 17–23.

[13] L.A. Bereschenko, H. Prummel, G.J. Euverink, A.J. Stams, M.C. Loosdrecht, Effect of conventional chemical treatment on the microbial population in a biofouling layer of reverse osmosis systems, Water Res., 45 (2011) 405–416.

[14] Q. Li, M. Elimelech, Synergistic effects in combined fouling of a loose nanofiltration membrane by colloidal materials and natural organic matter, J. Membr. Sci., 278 (2006) 72–82.

[15] I. Demir, M.E. Pasaoglu, S. Guclu, T. Turken, S. Yildiz, V. Balahorli, I. Koyuncu, Foulant and chemical cleaning analysis of ultra filtration membrane used in landfill leachate treatment, Desal. Water Treat., 77 (2017) 142–148.

[16] H.C. Flemming, G. Schaule, Biofouling on membranes - A microbiological approach, Desalination, 70 (1988) 95–119.

[17] H.C. Flemming, G. Schaule, T. Griebe, J. Schmitt, A. Tamachkiarowa, Biofouling—the achilles heel of membrane processes, Desalination, 113 (1997) 215–225.

[18] S. Efrima, L. Zeiri, Under standing SERS of bacteria, J. Raman Spectrosc., 40 (2009) 277–288.

[19] S. Nie, S.R. Emory, Probing single molecules and single nanoparticles by surface-enhanced Raman scattering, Science, 275 (1997) 1102–1106.

[20] N.P. Ivleva, M. Wagner, A. Szkola, H. Horn, R. Niessner, C. Haisch, Label-free in situ SERS imaging of biofilms, J. Phys. Chem. B., 114 (2010) 10184–10194.

[21] Y. Chao, T. Zhang, Surface-enhanced raman scattering (SERS) revealing chemical variation during biofilm formation: from initial attachment to mature biofilm, Anal. Bioanal. Chem., 404 (2012) 1465–1475.

[22] L. Cui, M. Yao, B. Ren, K.S. Zhang, Sensitive and versatile detection of the fouling process and fouling propensity of proteins on polyvinylidene fluoride membranes via surface-enhanced raman spectroscopy, Anal. Chem., 83 (2011) 1709–1716.

[23] P.Y. Chen, L. Cui, K.S. Zhang, Surface-enhanced Raman spectroscopy monitoring the development of dual-species biofouling on membrane surfaces, J. Membr. Sci., 473 (2015) 36–44.

[24] G. Frens, Z. Kolloid, J. Turkevich, J. Hillier, P.C. Stevenson, Controlled nucleation for the regulation of the particle size in mono disperse gold suspensions, Nature Phys. Sci., 241 (1973) 20–22.

[25] L. Cui, P.Y. Chen, S.D. Chen, Z.H. Yuan, C.P. Yu, B. Ren, K.S. Zhang, In situ study of the antibacterial activity and mechanism of action of silver nanoparticles by surface-enhanced Raman spectroscopy, Anal. Chem., 85 (2013) 5436–5443.

[26] L. Cui, S.D. Chen, K.S. Zhang, Effect of toxicity of Ag nanoparticles on SERS spectral variance of bacteria, Spectrochim. Acta, Part A, 137 (2015) 1061–1066.

[27] F.L. Martin, J.G. Kelly, V. Llabjani, P.L. Martin-Hirsch, I.I. Patel, J. Trevisan, N.J. Fullwood, M.J. Walsh, Distinguishing cell types or populations based on the computational analysis of their infrared spectra, Nat. Protoc., 5 (2010) 1748–1760.

[28] M. Herzberg, D. Berry, L. Raskin, Impact of micro filtration treatment of secondary wastewater effluent on biofouling of reverse osmosis membranes, Water Res., 44 (2010) 167–176.

[29] E.M. Hoek, M. Elimelech, Cake-enhanced concentration polarization: a new fouling mechanism for salt-rejecting membranes, Environ. Sci. Technol., 37 (2003) 5581–5588.

[30] S. Lee, J. Cho, M. Elimelech, Combined influence of natural organic matter (NOM) and colloidal particles on nanofiltration membrane fouling, J. Membr. Sci., 262 (2005) 27–41.

[31] H. Ng, M. Elimelech, Influence of colloidal fouling on rejection of trace organic contaminants by reverse osmosis, J. Membr. Sci., 244 (2004) 215–226.

[32] Q. Li, Z. Xu, I. Pinnau, Fouling of reverse osmosis membranes by biopolymers in wastewater secondary effluent: Role of membrane surface properties and initial permeate flux, J. Membr. Sci., 290 (2007) 173–181.

[33] M. Herzberg, S. Kang, M. Elimelech, Role of extracellular polymeric substances (EPS) in biofouling of reverse osmosis membranes, Environ. Sci. Technol., 43 (2009) 4393–4398.

[34] W.S. Ang, S. Lee, M. Elimelech, Chemical and physical aspects of cleaning of organic-fouled reverse osmosis membranes, J. Membr. Sci., 272 (2006) 198–210.

[35] W. Ang, M. Elimelech, Protein (BSA) fouling of reverse osmosis membranes: Implications for wastewater reclamation, J. Membr. Sci., 296 (2007) 83–92.

[36] L.A. Bereschenko, A.J. Stams, G.J. Euverink, M.C. Loosdrecht, Biofilm formation on reverse osmosis membranes is initiated and dominated by Sphingomonas spp, Appl. Environ. Microbiol., 76 (2010) 2623–2632.

[37] Y. Baek, J. Yu, S.H. Kim, S. Lee, J. Yoon, Effect of surface properties of reverse osmosis membranes on biofouling occurrence under filtration conditions, J. Membr. Sci., 382 (2011) 91–99.

[38] W. Lee, C.H. Ahn, S. Hong, S. Kim, S. Lee, Y. Baek, J. Yoon, Evaluation of surface properties of reverse osmosis membranes on the initial biofouling stages under no filtration condition, J. Membr. Sci., 351 (2010) 112–122.

[39] J.S. Andrews, S.A. Rolfe, W.E. Huang, J.D. Scholes, S.A. Banwart, Biofilm formation in environmental bacteria is influenced by different macromolecules depending on genus and species, Environ. Microbiol., 12 (2010) 2496–2507.

[40] H.C. Flemming, J. Wingender, The biofilm matrix, Nat. Rev. Microbiol., 8 (2010) 623–633.

[41] C.B. Whitchurch, T. Tolker-Nielsen, P.C. Ragas, J.S. Mattick, Extracellular DNA required for bacterial biofilm formation, Science, 295 (2002) 1487.

[42] W.T. Cheng, M.T. Liu, H.N. Liu, S.Y. Lin, Micro-Raman spectroscopy used to identify and grade human skin pilomatrixoma, Microsc. Res. Tech., 68 (2005) 75–79.

[43] Z. Huang, H. Lui, D.I. McLean, M. Korbelik, H. Zeng, Raman spectroscopy in combination with background near-infrared autofluorescence enhances the in vivo assessment of malignant tissues, Photochem. Photobiol., 81 (2005) 1219–1226.

[44] A. Conrad, M.K. Suutari, M.M. Keinanen, A. Cadoret, P. Faure, L. Mansuy-Huault, J.C. Block, Fatty acids of lipid fractions in extracellular polymeric substances of activated sludge flocs, Lipids, 38 (2003) 1093–1105.

[45] B. Frølund, R. Palmgren, K. Keiding, P.H. Nielsen, Extraction of extracellular polymers from activated sludge using a cation exchange resin, Water Res., 30 (1996) 1749–1758.

[46] K. Kimura, Y. Oki, Efficient control of membrane fouling in MF by removal of biopolymers: Comparison of various pretreatments, Water Res., 115 (2017) 172–179.

[47] J.W. Chan, D.S. Taylor, T. Zwerdling, S.M. Lane, K. Ihara, T. Huser, Micro-Raman spectroscopy detects individual neoplastic and normal hematopoietic cells, Biophys. J., 90 (2006) 648–656.

[48] X. Li, T. Yang, S. Lib, T. Yu, Surface-enhanced Raman spectroscopy differences of saliva between lung cancer patients and normal people, European Conference on Biomedical Optics. Optical Society of America, 2011.